J|A|C|S ARTICLES

Published on Web 08/24/2009

Conjugated Polymer/Porphyrin Complexes for Efficient Energy Transfer and Improving Light-Activated Antibacterial Activity

Chengfen Xing, Qingling Xu, Hongwei Tang, Libing Liu,* and Shu Wang*

Beijing National Laboratory for Molecular Sciences, Key Laboratory of Organic Solids, Institute of Chemistry, Chinese Academy of Sciences, Beijing, 100190, People's Republic of China

Received June 3, 2009; E-mail: wangshu@iccas.ac.cn; liulibing@iccas.ac.cn

Abstract: With the increasing antibiotic resistance of microorganisms, there is a growing interest in the design and development of new materials that are effective in killing bacteria to replace conventional antibiotics. Herein, a new anionic water-soluble polythiophene (PTP) and a cationic porphyrin (TPPN) are synthesized and characterized. They can form a complex through electrostatic interactions, and efficient energy transfer from PTP to TPPN occurs upon irradiation under white light (400−800 nm). The energy of TPPN transfers to triplet by intersystem crossing, followed by sensitization of oxygen molecule to enhance the efficiency of singlet oxygen generation related to TPPN itself. The positive charges of PTP/TPPN complex promote its adsorption to the negatively charged bacteria membranes of Gram-negative *Escherichia coli* and Gram-positive *Bacillus subtilis* through electrostatic interactions, and the singlet oxygen effectively kills the bacteria. The photosensitized inactivation of bacteria for the PTP/TPPN complex is efficient, and about 70% reduction of bacterial viability is observed after only 5 min of irradiation with white light at a fluence rate of 90 mW·cm^{-2} (27 J·cm^{-2}). The technique provides a promising application in photodynamic inactivation of bacteria on the basis of enhanced energy transfer offered by light-harvesting conjugated polymers.

Introduction

With the increasing antibiotic resistance of microorganisms, there is a growing interest in the design and development of new materials that are effective in killing bacteria to replace conventional antibiotics. Several biocidal materials such as nanoparticles,[1−3] carbon nanotubes,[4] and polymers containing pendant organic functionalities[5−8] have been tested in antibacterial therapies. Photodynamic antimicrobial chemotherapy (PACT) is a very promising approach for killing bacteria.[9,10] It is well-established that singlet oxygen ($^1O_2$) is produced as the main species responsible for cell death in PACT, and it seems probable that the initially generated singlet oxygen interacts with some component of the cell to produce reactive oxygen species.[11,12] Porphyrins are commonly used as the photosensitizers that can produce reactive oxygen species (in particular, $^1O_2$) upon exposure to light in the presence of oxygen.[13−16] However, most porphyrins are not broad-spectrum, exhibiting efficient antimicrobial activity against Gram-positive rather than Gram-negative bacteria.[11] The resistance of Gram-negative bacteria to a variety of porphyrins is related to the presence of a highly organized outer membrane in these bacteria, limiting their interactions with porphyrins and intercepting $^1O_2$. Cationic porphyrins can bind to negatively charged outer membrane of Gram-negative bacteria and efficiently enable the photoinactivation of the bacteria.[15,17] In recent years, light-harvesting dendrimers containing multiple donor-absorbing chromophores and a central porphyrin acceptor have been developed to extend

(1) Zhang, H.; Wang, D.; Butler, R.; Campbell, N.; Long, J.; Tan, B.; Duncalf, D. J.; Foster, A. J.; Hopkinson, A.; Taylor, D.; Angus, D.; Cooper, A. I.; Rannard, S. P. *Nat. Nanotechnol.* **2008**, *3*, 506–511.
(2) Panáček, A.; Kvítek, L.; Prucek, R.; Kolář, M.; Večeřová, R.; Pizúrová, N.; Sharma, V. K.; Nevěčná, T.; Zbořil, R. *J. Phys. Chem. B* **2006**, *110*, 16248–16253.
(3) Narband, N.; Mubarak, M.; Ready, D.; Parkin, I. P.; Nair, S. P.; Green, M. A.; Beeby, A.; Wilson, M. *Nanotechnology* **2008**, *19*, 445102.
(4) Kang, S.; Pinault, M.; Pfefferle, L. D.; Elimelech, M. *Langmuir* **2007**, *23*, 8670–8673.
(5) Parsons, C.; McCoy, C. P.; Gorman, S. P.; Jones, D. S.; Bell, S. E. J.; Brady, C.; McGlinchey, S. M. *Biomaterials* **2009**, *30*, 597–602.
(6) Thorsteinsson, T.; Másson, M.; Kristinsson, K. G.; Hjálmarsdóttir, M. A.; Hilmarsson, H.; Loftsson, T. *J. Med. Chem.* **2003**, *46*, 4173–4181.
(7) Huang, J.; Murata, H.; Koepsel, R. R.; Russell, A. J.; Matyjaszewski, K. *Biomacromolecules* **2007**, *8*, 1396–1399.
(8) Gabriel, G. J.; Pool, J. G.; Som, A.; Dabkowski, J. M.; Coughlin, E. B.; Muthukumar, M.; Tew, G. N. *Langmuir* **2008**, *24*, 12489–12495.
(9) Konig, K.; Teschke, M.; Sigusch, B.; Glockmann, E.; Eick, S.; Pfister, W. *Cell. Mol. Biol.* **2000**, *46*, 1297–1303.
(10) Dolmans, D. E.; Fukumura, D.; Jain, R. K. *Nat. Rev. Cancer* **2003**, *3*, 380–387.
(11) Bonnett, R.; Buckley, D. G.; Burrow, T.; Galia, A. B. B.; Saville, B.; Songca, S. P. *J. Mater. Chem.* **1993**, *3*, 323–324.
(12) Maisch, T.; Baier, J.; Franz, B.; Maier, M.; Landthaler, M.; Szeimies, R.-M.; Baumler, W. *Proc. Natl. Acad. Sci. U.S.A.* **2007**, *104*, 7223–7228.
(13) Tomé, J. P. C.; Neves, M. G. P. M. S.; Tomé, A. C.; Cavaleiro, J. A. S.; Soncin, M.; Magaraggia, M.; Ferro, S.; Jori, G. *J. Med. Chem.* **2004**, *47*, 6649–6652.
(14) Caminos, D. A.; Spesia, M. B.; Durantini, E. N. *Photochem. Photobiol. Sci.* **2006**, *5*, 56–65.
(15) Costa, L.; Alves, E.; Carvalho, C. M. B.; Tomé, J. P. C.; Faustino, M. A. F.; Neves, M. G. P. M. S.; Tomé, A. C.; Cavaleiro, J. A. S.; Cunha, Â.; Almeida, A. *Photochem. Photobiol. Sci.* **2008**, *7*, 415–422.
(16) Caminos, D. A.; Durantini, E. N. *Bioorg. Med. Chem.* **2006**, *14*, 4253–4259.
(17) Nitzan, Y.; Ashkenazi, H. *Curr. Microbiol.* **2001**, *42*, 408–414.

the spectrum range of photosensitizers and enhance $^1O_2$ generation by fluorescence resonance energy transfer (FRET).[18−21] Quantum dots,[22] gold and silica nanoparticles[23] modified with porphyrin photosensitizer, were also developed to undergo energy transfer and to generate $^1O_2$. For the preparation of these systems, complex synthesis or modification procedures are required. To overcome this limit, polymer micelles encapsulating porphyrin were prepared to induce $^1O_2$ production by the FRET mechanism.[24] Although these materials have good potential as photosensitizers, they are not studied for PACT experiments.

Water-soluble conjugated polymers (CPs) are known to have light-harvesting properties and can coordinate the action of a large number of absorbing units.[25,26] The excitation energy along the backbone of CP transferring to the energy/electron acceptor results in the amplification of optical signals. CPs have been utilized in sensitive detection of biomacromolecules (nucleic acids and proteins) and fluorescence imaging.[27−39] Recent works have shown that the cationic conjugated polymers can bind to the surface of bacteria and function as singlet oxygen photosensitizers to kill the bacteria with irradiation under white light.[40−42] In this paper, we present a new design of electrostatic complex of water-soluble anionic conjugated polymer with cationic porphyrin, in which positive charges on the complex can promote tight electrostatic interactions with negatively charged sites at the surface of Gram-negative or Gram-positive bacteria to exhibit efficient antibacterial activity. The electrostatic complex has three significant characteristics. First, through electrostatic interactions, anionic conjugated polymer can form a complex with cationic porphyrin, and it does not require covalent linkage of the porphyrin moiety to the backbone or side chain of conjugated polymer,[43] which reduces complicated synthesis procedures. Second, efficient energy transfer from conjugated polymer to porphyrin followed by intersystem crossing to porphyrin triplet and sensitization of oxygen molecule enhances the efficiency of $^1O_2$ generation. Third, in comparison to porphyrin itself, the use of light-harvesting conjugated polymer reduces the irradiation time while retaining efficient antibacterial activity.

Scheme 1. Schematic Antibacterial Mechanism of PTP/TPPN Complex and Chemical Structures of PTP and TPPN. ET = energy transfer

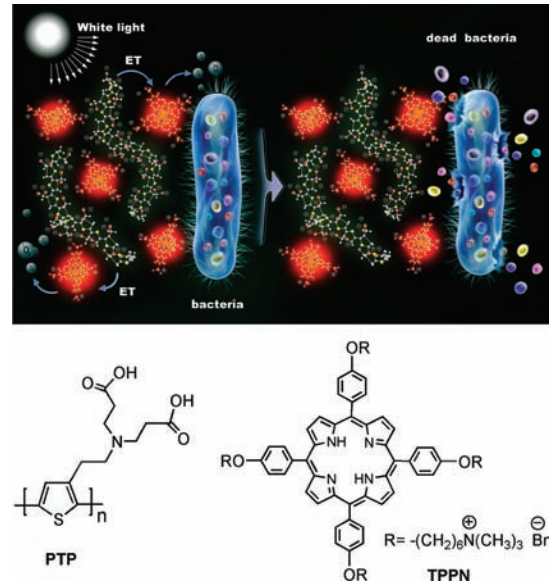

Results and Discussion

Anionic water-soluble conjugated polythiophene derivative (PTP) and cationic 5,10,15,20-tetrakis[4-(6-*N*,*N*,*N*-trimethylammoniumhexyloxy)phenyl]porphyrin bromide (TPPN) were synthesized for preparing the PTP/TPPN complex through electrostatic interactions (see Scheme 1 for their chemical structures). The antibacterial mechanism of PTP/TPPN complex is illustrated in Scheme 1. The cationic TPPN binds to anionic polymer PTP, and the cationic PTP/TPPN complex can bind to negatively charged sites at the membrane surface of Gram-negative bacteria by tight electrostatic interactions. Upon irradiation under white light (400−800 nm), both PTP and TPPN are excited while the excitation energy of PTP transfers to TPPN. Because there is no overlap integral between PTP and TPPN, energy transfer between them may originate from their orbital interactions by the Dexter mechanism rather than the Förster mechanism.[44] The energy of TPPN transfers to triplet

(18) Dichtel, W. R.; Serin, J. M.; Edder, C.; Fréchet, J. M. J.; Matuszewski, M.; Tan, L.-S.; Ohulchanskyy, T. Y.; Prasad, P. N. *J. Am. Chem. Soc.* **2004**, *126*, 5380–5381.
(19) Oar, M. A.; Dichtel, W. R.; Serin, J. M.; Fréchet, J. M. J.; Rogers, J. E.; Slagle, J. E.; Fleitz, P. A.; Tan, L.-S.; Ohulchanskyy, T. Y.; Prasad, P. N. *Chem. Mater.* **2006**, *18*, 3682–3692.
(20) Ishi-i, T.; Taguri, Y.; Kato, S.; Shigeiwa, M.; Gorohmaru, H.; Maeda, S.; Mataka, S. *J. Mater. Chem.* **2007**, *17*, 3341–3346.
(21) Briñas, R. P.; Troxler, T.; Hochstrasser, R. M.; Vinogradov, S. A. *J. Am. Chem. Soc.* **2005**, *127*, 11851–11862.
(22) Tsay, J. M.; Trzoss, M.; Shi, L.; Kong, X.; Selke, M.; Jung, M. E.; Weiss, S. *J. Am. Chem. Soc.* **2007**, *129*, 6865–6871.
(23) Kim, S.; Ohulchanskyy, T. Y.; Pudavar, H. E.; Pandey, R. K.; Prasad, P. N. *J. Am. Chem. Soc.* **2007**, *129*, 2669–2675.
(24) Chen, C.-Y.; Tian, Y.; Cheng, Y.-J.; Young, A. C.; Ka, J.-W.; Jen, A. K.-Y. *J. Am. Chem. Soc.* **2007**, *129*, 7220–7221.
(25) Thomas, S. W., III; Joly, G. D.; Swager, T. M. *Chem. Rev.* **2007**, *107*, 1339–1386.
(26) Liu, B.; Bazan, G. C. *Chem. Mater.* **2004**, *16*, 4467–4476.
(27) Ho, H. A.; Najari, A.; Leclerc, M. *Acc. Chem. Res.* **2008**, *41*, 168–178.
(28) Gaylord, B. S.; Heeger, A. J.; Bazan, G. C. *Proc. Natl. Acid. Sci. U.S.A.* **2002**, *99*, 10954–10957.
(29) Bunz, U. H. F. *Chem. Rev.* **2000**, *100*, 1605–1644.
(30) Pinto, M. R.; Schanze, K. S. *Proc. Natl. Acad. Soc. U.S.A.* **2004**, *101*, 7505–7510.
(31) Achyuthan, K. E.; Bergstedt, T. S.; Chen, L.; Jones, R. M.; Kumaraswamy, S.; Kushon, S. A.; Ley, K. D.; Lu, L.; McBranch, D.; Mukundan, H.; Rininsland, F.; Shi, X.; Xia, W.; Whitten, D. G. *J. Mater. Chem.* **2005**, *15*, 2648–2656.
(32) Nilsson, K. P. R.; Inganäs, O. *Nat. Mater.* **2003**, *2*, 419–424.
(33) Feng, F.; He, F.; An, L.; Wang, S.; Li, Y.; Zhu, D. *Adv. Mater.* **2008**, *20*, 2959–2964.
(34) Feng, F.; Wang, H.; Han, L.; Wang, S. *J. Am. Chem. Soc.* **2008**, *130*, 11338–11343.
(35) Feng, F.; Tang, Y.; Wang, S.; Li, Y.; Zhu, D. *Angew. Chem., Int. Ed.* **2007**, *46*, 7882–7886.
(36) McRae, R. L.; Phillips, R. L.; Kim, I.-B.; Bunz, U. H. F.; Fahrni, C. J. *J. Am. Chem. Soc.* **2008**, *130*, 7851–7853.
(37) Björk, P.; Nilsson, K. P. R.; Lenner, L.; Kågedal, B.; Persson, B.; Inganäs, O.; Jonasson, J. *Mol. Cell. Probes* **2007**, *21*, 329–337.
(38) Sigurdson, C. J.; Nilsson, K. P. R.; Hornemann, S.; Manco, G.; Polymenidou, M.; Schwarz, P.; Leclerc, M.; Hammarström, P.; Wüthrich, K.; Aguzzi, A. *Nat. Methods* **2007**, *4*, 1023–1030.
(39) Ren, X. S.; Xu, Q. H. *Langmuir* **2009**, *25*, 43–47.
(40) Lu, L.; Rininsland, F. H.; Wittenburg, S. K.; Achyuthan, K. E.; McBranch, D. W.; Whitten, D. G. *Langmuir* **2005**, *21*, 10154–10159.
(41) Chemburu, S.; Corbitt, T. S.; Ista, L. K.; Ji, E.; Fulghum, J.; Lopez, G. P.; Ogawa, K.; Schanze, K. S.; Whitten, D. G. *Langmuir* **2008**, *24*, 11053–11062.
(42) Corbitt, T. S.; Sommer, J. R.; Chemburu, S.; Ogawa, K.; Ista, L. K.; Lopez, G. P.; Whitten, D. G.; Schanze, K. S. *Appl. Mater. Interfaces* **2009**, *1*, 48–52.
(43) Wu, C. L.; Xu, Q. H. *Macromol. Rapid Commun.* **2009**, *30*, 504–508.
(44) Lakowicz, J. R. *Principles of Fluorescence Spectroscopy*; Kluwer Academic/Plenum: New York, 1999.

Scheme 2. Synthetic Routes to PTP and TPPN

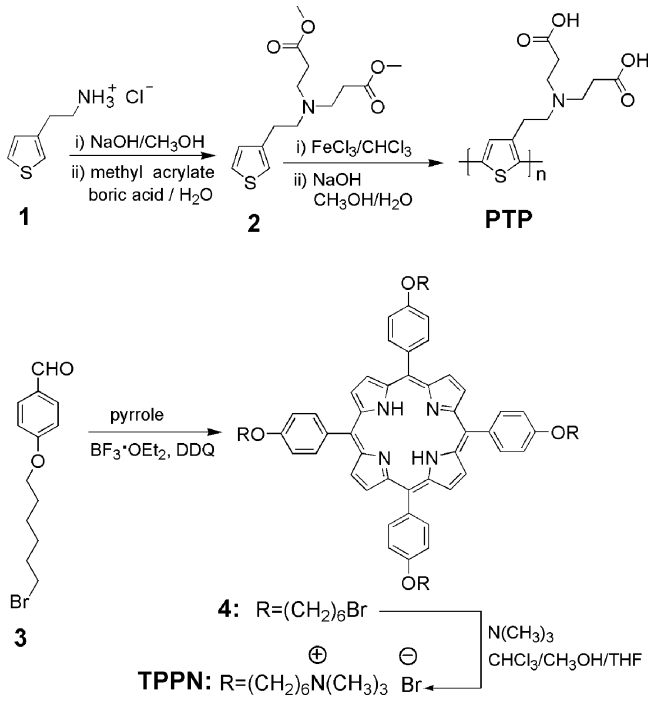

by intersystem crossing followed by sensitization of the oxygen molecule to enhance the efficiency of $^1O_2$ generation related to TPPN itself. Therefore, the Gram-negative bacteria bound to PTP/TPPN complex are efficiently killed by the produced $^1O_2$.

Procedures for the synthesis of PTP and TPPN are outlined in Scheme 2. The monomer **2** was prepared by reacting 2-(3-thienyl)ethylamine[45] and methyl acrylate in the presence of boric acid with a yield of 56%. PTP was obtained through oxidative polymerization of monomer **2** in chloroform by use of $FeCl_3$ as oxidizing agent followed by hydrolysis in NaOH aqueous solution and dialysis in water through a membrane with molecular weight cutoff of 3500 g/mL. Reaction of pyrrole and 4-(6-bromohexyloxy)benzaldehyde (**3**)[46] in the presence of BF_3−diethyl ether in $CHCl_3$ was followed by treatment with DDQ to afford porphyrin derivative **4** with a yield of 12%. Compound **4** was treated with 30% trimethylamine−methanol solution to obtain cationic TPPN with a yield of 72%.

The morphology of PTP/TPPN complex was studied by fluorescence microscopy. As shown in Figure 1a,b, the dot-like aggregates were observed for the complex driven by electrostatic interactions between oppositely charged PTP and TPPN. The size of aggregates was 1−4 μm. The photophysical properties of PTP and TPPN were investigated in phosphate-buffered saline (PBS; 20 mM, pH 7.4) as shown in Figure 1c,d. PTP exhibited an absorption maximum at 410 nm, corresponding to the $\pi-\pi^*$ transition of conjugated units, with an extinction coefficient of 6.7×10^3 $M^{-1}\cdot cm^{-1}$. The emission maximum peak was 561 nm for PTP with fluorescence quantum efficiency of 4.8%. The absorption spectra of TPPN in PBS buffer exhibited a Soret band around 420 nm and Q bands between 520 and 670 nm. TPPN exhibited an emission maximum at 655 nm with fluorescence quantum efficiency of 3.5%. Irradiation at 470 nm selectively excited PTP; the PTP emission was completely quenched ([PTP] = 9.0 μM in repeat units (RUs), [TPPN] = 3.0 μM), and emission was seen predominantly from TPPN, where the energy transfer efficiency is 96% calculated by the quenching of PTP emission. Actually, the aggregation of PTP/TPPN complex keeps them in close proximity, allowing for efficient energy transfer. TPPN showed 2-fold enhanced emission in the presence of PTP in comparison to the case without PTP with excitation of 420 nm, which is due to optical amplification by the conjugated polymers.

The fluorescence quenching of PTP ([PTP] = 9.0 μM in repeat units, RUs) by TPPN was performed in PBS buffer. The excitation wavelength was chosen at 470 nm, where PTP was selectively excited. As shown in Figure 1e, the fluorescence intensity of PTP was gradually decreased with increasing amounts of TPPN and the emission of TPPN at 655 nm enhanced gradually. The quenching efficiency was related to the Stern−Volmer constant (K_{SV}) and was determined by monitoring measurable changes in the fluorescence of PTP via the Stern−Volmer equation (eq 1):[46]

$$I_0/I = 1 + K_{SV}[Q] \quad (1)$$

At low concentrations of TPPN (0−1.5 μM), a linear Stern−Volmer plot was obtained with a K_{SV} value of 5.58×10^6 M^{-1} (Figure 1f), which indicated the superquenching behavior of PTP by TPPN. The quenching of PTP by TPPN shows downward curvature at higher TPPN concentration (>3.0 μM), which indicates that not all TPPN molecules are accessible by electrostatic interactions to PTP in this case.

The generation of $^1O_2$ can be probed by disodium salt of 9,10-anthracenedipropionic acid (ADPA),[47] where the ADPA converts to its endoperoxide in the presence of $^1O_2$, leading to the decrease of ADPA absorption maximum around 378 nm. As shown in Figure 2a, the generation ability of $^1O_2$ by PTP/TPPN complex was evaluated upon exposure to white light. TPPN or PTP alone was also employed as the control experiment. The first-order plots of the decrease of ADPA absorption at 378 nm as a function of the irradiation time showed that less ADPA absorption intensity change was observed for TPPN or PTP itself throughout the time, while a noticeable decrease in the ADPA absorbance for PTP/TPPN complex was observed. Therefore, the energy transfer from PTP to TPPN contributed significantly to $^1O_2$ generation. As the energy transfer from PTP to TPPN was dependent on their concentration ratios in buffer solution, the $^1O_2$ generation as a function of concentration ratio was also evaluated by the ADPA probe. Figure 2b showed time curves of the absorbance decrease of ADPA at a fixed concentration of TPPN ([TPPN] = 3.0 μM) with PTP varying from 1.0 to 12.0 μM. As shown in Figure 2c, the bleaching rate constants (K_{obs}) of ADPA in the presence of TPPN, PTP, and PTP/TPPN were 2.85×10^{-4} s^{-1}, 1.25×10^{-3} s^{-1}, and 2.73×10^{-3} s^{-1}, respectively. The bleaching rate for PTP/TPPN complex was 9.6-fold faster than that for TPPN and 2.2-fold faster than that for PTP. It was found that the bleaching rate of ADPA enhanced with increasing concentration of PTP and reached a plateau after 9.0 μM in RU (the concentration ratio of PTP to TPPN is 3.0). These results gave more evidence that the energy transfer from PTP enhanced the $^1O_2$ generation ability of TPPN. The polymer PTP as a donor transfers its excited-state energy to the acceptor (TPPN) via energy transfer, where enhanced intersystem cross-

(45) Tang, Y.; He, F.; Yu, M.; Feng, F.; An., L.; Sun, H.; Wang, S.; Li, Y.; Zhu, D. *Macromol. Rapid Commun.* **2006**, *27*, 389–392.
(46) Kim, O.-K.; Je, J.; Melinger, J. S. *J. Am. Chem. Soc.* **2006**, *128*, 4532–4533.
(47) Lindig, B. A.; Rodgers, M. A. J.; Schaap, A. P. *J. Am. Chem. Soc.* **1980**, *102*, 5590–5593.

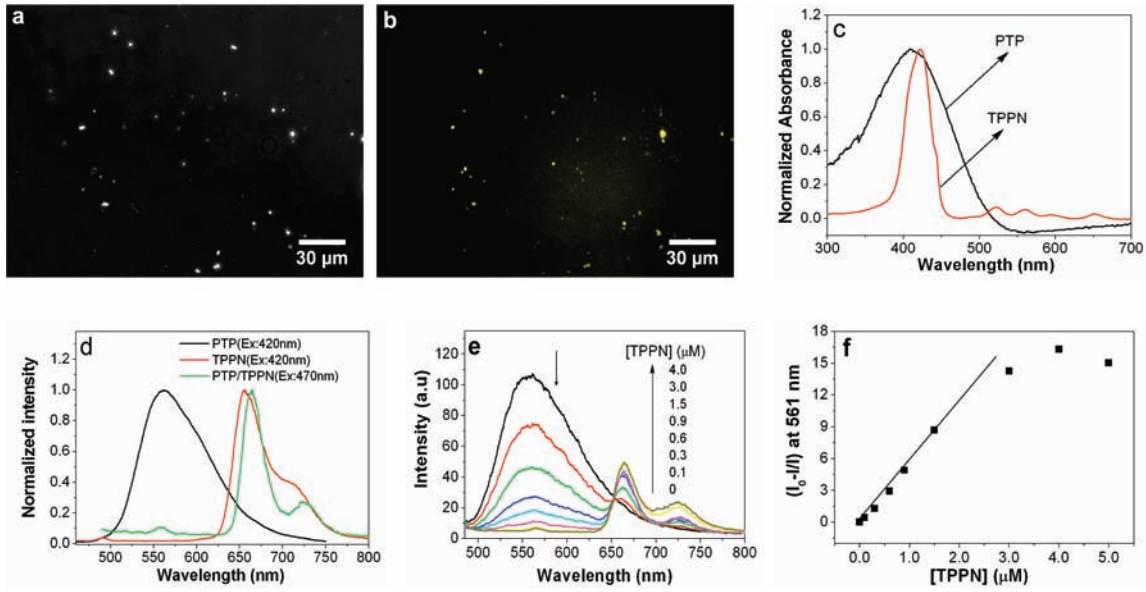

Figure 1. Morphology of PTP/TPPN complex and photophysical properties of PTP and TPPN. (a) Phase-contrast images and (b) fluorescence microscope images of PTP/TPPN complex in buffer solution are shown. [PTP] = 36.0 μM in RUs, [TPPN] = 12.0 μM. The phase contrast images were taken at 100 ms and the fluorescence images were taken via fluorescence microscopy at 4500 ms exposure time. The false color is yellow and the type of light filter is D455/70 nm exciter, 500 nm beamsplitter, and D525/30 nm emitter. Magnification of object lens is 40×. (c) Normalized UV−vis absorption spectra of PTP and TPPN. (d) Normalized emission spectra of PTP, TPPN, and PTP /TPPN complex. (e) Fluorescence emission spectra of PTP in buffer solution with successive additions of TPPN. (f) K_{SV} plot of PTP in the presence of TPPN. [PTP] = 9.0 μM in RUs, [TPPN] = 0−5.0 μM. The excitation wavelength is 470 nm.

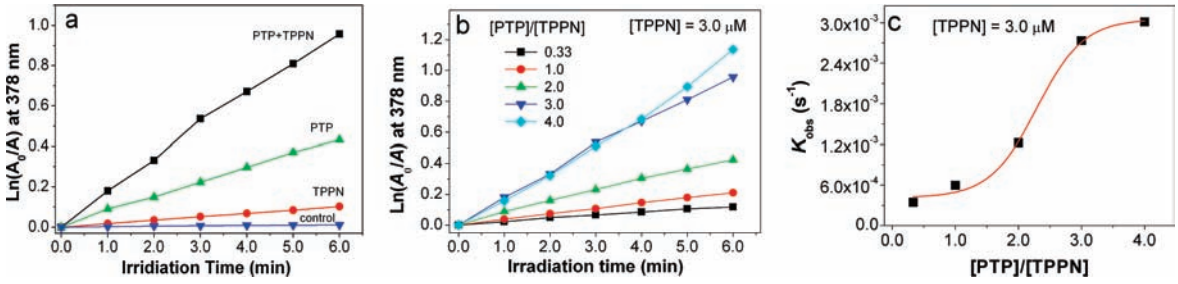

Figure 2. Bleaching rate constants (K_{obs}) of ADPA in the presence of TPPN, PTP, and PTP/TPPN. (a) First-order plots for the decrease of ADPA absorption at 378 nm as a function of irradiation time in the presence of TPPN, PTP, and PTP/TPPN complex ([PTP]/[TPPN] = 3.0) in PBS buffer solution. [TPPN] = 3.0 μM, [PTP] = 9.0 μM in RUs, and [ADPA] = 60 μM. The control plot was with only light for PTP/TPPN without ADPA. (b) First-order plots for the bleaching of ADPA for PTP/TPPN complex versus irradiation time at a fixed concentration of TPPN with varying PTP concentrations. [TPPN] = 3.0 μM, [PTP] = 1.0−12.0 μM in RU, and [ADPA] = 60.0 μM. (c) Dependence of the bleaching rate of ADPA for PTP/TPPN complex on the concentration ratio of PTP to TPPN with a fixed concentration of TPPN. [TPPN] = 3.0 μM, [PTP] = 1.0−12.0 μM in RU, [ADPA] = 60.0 μM. The H_2O in buffer solution was replaced by D_2O. A_0 is the absorbance of ADPA at 378 nm before irradiation, and A is that after irradiation. Values represent subtraction of the residual bleaching data of ADPA alone under the same irradiation condition. White light was used for the irradiation experiments.

ing in the complex occurs and produces a long-lived triplet state of TPPN. The TPPN triplet sensitizes ground-state oxygen molecule to generate $^1O_2$.

The antibacterial activity of PTP/TPPN complex toward Gram-negative bacteria *E. coli* in the dark and upon white-light illumination was studied by fluorescence microscopy. In these experiments, the *E. coli* suspension incubated with PTP/TPPN complex was exposed to white light and then ethidium bromide (EB) was added to stain apoptotic or dead bacterial cells. Figure 3a−d shows the overlapping images of *E. coli* suspensions under the phase contrast bright-field and under the fluorescence field, where bacterial death was indicated by the red fluorescence of EB. The results showed that the PTP/TPPN complex exhibited efficient biocidal activity for living *E. coli* in comparison with TPPN or PTP alone.

Bacterial survival experiments upon exposure to white light were also done by a traditional surface plating method (Figure 4a,b). Colony counting showed that the killing efficiency upon irradiation of *E. coli* suspension incubated with PTP/TPPN ([PTP] = 9.0 μM in RUs, [TPPN] = 3.0 μM) was ~70%, whereas the killing efficiencies for TPPN and PTP alone were below 15% (Figure 4c). In the control experiments, killing efficiencies of less than 10% were obtained for PTP/TPPN complex, TPPN, and PTP alone in the dark. Studies of the effect of PTP concentrations on killing efficiency toward *E. coli* under irradiation at a fixed concentration of TPPN ([TPPN] = 3.0 μM) showed that the killing efficiency enhanced with increasing concentration of PTP and reached a plateau after 9.0 μM in RUs (Figure 4d). Comparison of both absolute and relative $^1O_2$ production rates as well as reduction in cell viability percentage for TPPN, PTP, and PTP/TPPN has been tabulated to show the synergistic effects (Table 1). The results were consistent with the generation ability of $^1O_2$ for PTP/TPPN complex as shown in Figure 2 and show that $^1O_2$ production enhancement is the main reason for the reduction in cell viability. Although ~70% kill efficiency is somewhat more modest than some reported

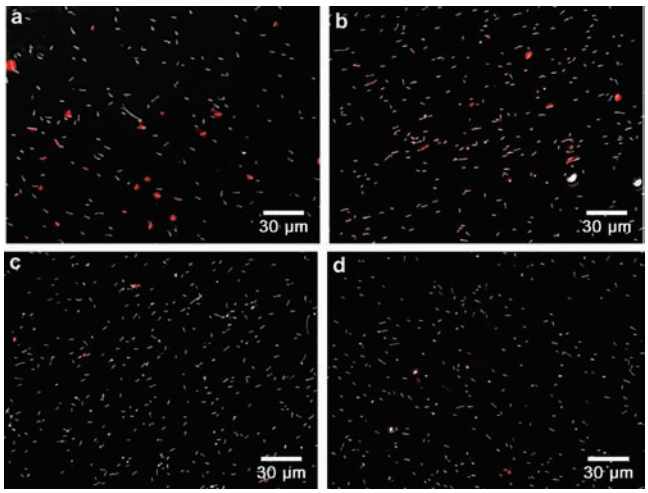

Figure 3. Antibacterial activity of PTP/TPPN complex toward Gram-negative bacteria *E. coli*. Overlapping images of *E. coli* suspensions under the phase contrast bright-field and under the fluorescence field incubated with (a) PTP/TPPN complex, (b) PTP, or (c) TPPN and (d) blank (without photosensitizer) under irradiation. *E. coli* was grown at 37 °C for 12 h, washed with PBS, and then incubated with photosensitizers for certain times in dark and exposed to the white light. Upon addition of EB to the samples, the phase contrast images were taken at 100 ms and the fluorescence images were taken via fluorescence microscopy at 5000 ms exposure time. The false color of EB is red and the type of light filter is D540/40 nm exciter, 570 nm beamsplitter, and D600/50 nm emitter. Magnification of object lens is 40×.

PACT systems that caused more than 90% reduction,[48] both the light energy and the irradiation time are more than those of our PTP/TPPN system.

To address the generality of our PTP/TPPN-based PACT technique, the reduction of cell viability of a Gram-positive bacterium, *Bacillus subtilis*, under irradiation of white light was also performed. The Gram-positive *B. subtilis* was more sensitive to photosensitizers than the Gram-negative *E. coli* due to the absence of outer cell membrane.[15,17] As shown in Figure 5, lower concentrations of PTP/TPPN ([TPPN] = 0.6 μM, [PTP] = 1.8 μM in RU) led to more than 90% reduction of cell viability toward *B. subtilis*. Furthermore, the PTP/TPPN complex exhibited efficient biocidal activity for living *B. subtilis* in comparison with TPPN or PTP alone, although the reduction in cell viability for TPPN reached ~36%.

It is demonstrated that the cationic porphyrins are more photoactive than anionic or nonionic ones toward Gram-negative bacteria,[15,17] although the singlet oxygen generation ability for these photosensitizers is similar. The presence of positive charges on antibacterial materials is mandatory.[48] To get more insight on the antibacterial activity of PTP and PTP/TPPN complex, their interactions with the bacterial cell surface were studied by fluorescence and phase contrast microscopy. As shown in Figure 6a,b, *E. coli* emitted yellow fluorescence upon treated with PTP/TPPN complex, which indicated that the bacteria were coated by the PTP/TPPN complex. For the case of negatively charged PTP itself, there was almost no adsorption to the *E. coli* surface, and thus the bacteria cells were not fluorescent (Figure 6c,d). The binding abilities of PTP and PTP/TPPN to *E. coli* were also estimated by comparing their emission intensity with and without interactions with *E. coli* in 2% sodium dodecyl sulfate (SDS). In these experiments, PTP or PTP/TPPN complex was incubated with *E. coli* in the dark followed by centrifuging (4000 rpm for 10 min) and washing with PBS buffer. The supernatant was removed and the bacteria were digested by SDS to give a homogeneous solution for fluorescence measurements with an excitation wavelength of 470 nm.[11,14] The fluorescence emission spectra of PTP and PTP/TPPN without incubation with *E. coli* in 2% SDS were taken as controls for comparison. As shown in Figure 6e, for PTP alone, its emission intensity decreased significantly after incubation with *E. coli*, suggesting that the anionic PTP has low binding affinity to *E. coli* cells. For PTP/TPPN complex, the PTP emission intensity changed slightly after incubation with *E. coli* (Figure 6f). These results showed that the PTP/TPPN complex has higher binding affinity to bacterial cells than the anionic PTP.

Furthermore, ζ potentials of the complex PTP/TPPN with and without *E. coli* have also been examined in phosphate-buffered saline (PBS, 20 mM, pH 7.4) (Figure 7). For PTP/TPPN/*E. coli*, ζ potentials became more cationic with increasing amounts of TPPN ([PTP] = 9.0 μM, [TPPN] = 0−6.0 μM), which confirmed the successful binding of PTP/TPPN to the *E. coli* surface (Figure 7a). For PTP, its surface charge density changes with varying concentration ratios of TPPN to PTP. ζ potentials data exhibited that the surface charges of PTP become cationic as the concentration ratio of TPPN to PTP was larger than 0.11 ([TPPN] = 1.0 μM, [PTP] = 9.0 μM in RU) (Figure 7b). Considering the antibacterial mode of PTP/TPPN complex, it appears that the positive charges of the complex promote its adsorption to the negative charged membrane of *E. coli* through electrostatic interactions, and then the singlet oxygen generated from the complex upon irradiation kills the *E. coli*. It was distance-dependent for the singlet oxygen to kill bacteria, and thus the antibacterial activity of PTP toward *E. coli* was lower than that of TPPN, although PTP can produce more singlet oxygen under irradiation than TPPN (Figure 2a).

Conclusion

In summary, the electrostatic complex of anionic water-soluble polythiophene and cationic porphyrin can be used to adsorb the Gram-negative and Gram-positive bacteria and generate singlet oxygen effectively to kill the bacteria under white light. This application takes advantage of the light-harvesting properties of conjugated polymers and the singlet oxygen generation nature of the energy transfer acceptor (porphyrin). The positive charges of complex promote its adsorption to the negatively charged membrane of *E. coli* through electrostatic interactions, and it was distance-dependent for the singlet oxygen to kill bacteria. The electrostatic complex has three significant characteristics. First, through electrostatic interactions, anionic conjugated polymer can form a complex with cationic porphyrin, and it does not require covalent linkage of porphyrin moiety to backbone or side chain of conjugated polymer, which reduces complicated synthesis procedures. Second, efficient energy transfer from conjugated polymer to porphyrin followed by intersystem crossing to porphyrin triplet and sensitization of oxygen molecule enhances the efficiency of singlet oxygen generation. Third, in comparison to porphyrin photosensitizer itself, the use of light-harvesting conjugated polymer reduces the irradiation time while retaining efficient antibacterial activity. About 70% reduction of bacterial viability is observed after only 5 min of irradiation with white light at a fluence rate of 90 mW·cm^{-2} (27 J·cm^{-2}). The technique provides a promising application in photodynamic inactivation

(48) Banfi, S.; Caruso, E.; Buccafurni, L.; Battini, V.; Zazzaron, S.; Barbieri, P.; Orlandi, V. *J. Photochem. Photobiol. B* **2006**, *85*, 28–38.

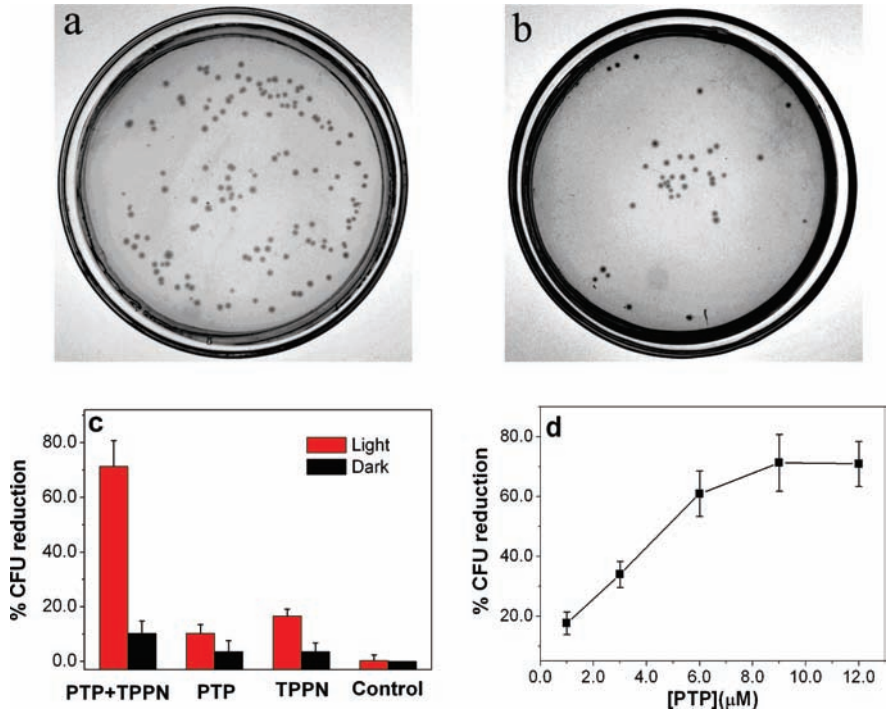

Figure 4. Number of colony forming units (cfu) for *E. coli* on LB agar plate. (a) Cfu control without photosensitizer in dark, (b) Cfu of *E. coli* suspension incubated with PTP/TPPN ([TPPN] = 3.0 μM, [PTP] = 9.0 μM in RUs) and irradiated with white light (27 J·cm^{-2}). Diameter of the solid LB agar plates was 90 mm. (c) Biocidal activity of PTP/TPPN, PTP, and TPPN toward *E. coli* in the dark and under white-light illumination for 5 min. [TPPN] = 3.0 μM, [PTP] = 9.0 μM in RUs. Dark and light control experiments were done with the cell suspensions irradiated or in the dark in the absence of photosensitizers. (d) Reduction of cell viability of PTP/TPPN complex toward *E. coli* as a function of PTP concentration. [TPPN] = 3.0 μM, [PTP] = 1.0−12.0 μM in RUs, [PTP]/ [TPPN] = 0.33−4.0. The white light dose was 27 J·cm^{-2} (irradiation for 5 min at a fluence rate of 90 mW cm^{-2}). Values represent means ± standard deviation of three separate experiments. Error bars represent standard deviations of data from three separate measurements.

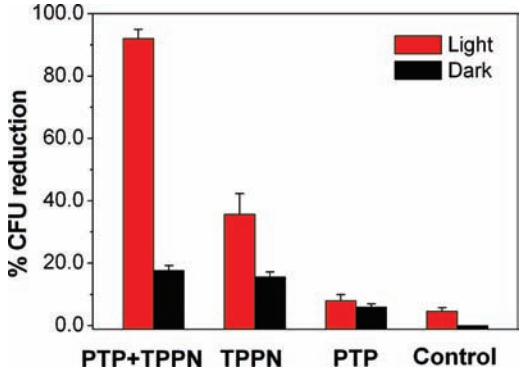

Figure 5. Biocidal activity of PTP/TPPN, PTP, and TPPN toward *B. subtilis* in the dark and under white-light irradiation for 5 min at a fluence rate of 90 mW·cm^{-2} (27 J·cm^{-2}). Control experiments were done with the cell suspensions irradiated or in the dark in the absence of photosensitizers. [TPPN] = 0.6 μM, [PTP] = 1.8 μM in RU. Error bars represent standard deviations of data from three separate measurements.

Table 1. Comparison of $^1O_2$ Production Rates and Cell Viability for TPPN, PTP, and PTP/TPPN

compd	K_{obs} (s^{-1})	relative K_{obs}	% cfu reduction	relative % cfu reduction
TPPN	2.85×10^{-4}	1.00	16.7	1.00
PTP	1.25×10^{-3}	4.38	10.3	0.62
PTP/TPPN	2.73×10^{-3}	9.58	71.3	4.28

of bacteria on the basis of enhanced energy transfer offered by light-harvesting conjugated polymers.

Experimental Section

Materials and Instruments. The disodium salt of 9,10-anthracenedipropionic acid (ADPA) was prepared according to the procedure in literature.[47] The bacteria *E. coli* was purchased from Tiangen Co. Ethidium bromide (EB) and sodium dodecyl sulfate (SDS) were purchased from Sigma. The ^{1}H NMR and ^{13}C NMR spectra were recorded on a Bruker Avance 400 MHz spectrometer. Elemental analyses were carried out with a Flash EA1112 instrument. The fluorescence spectra were measured on a Hitachi F-4500 fluorometer with a xenon lamp as excitation source. The excitation wavelength is 470 nm. UV−vis absorption spectra were taken on a Jasco V-550 spectrometer. Phase contrast bright-field and fluorescence images were taken with a fluorescence microscope (Olympus 1 × 71) with a mercury lamp (100 W) as light source. The excitation wavelength was 540/40 nm for EB. Experiments for photosensitized damage of bacteria were performed with a metal halogen lamp (Mejiro Genossen MVL-210) that simulated a white-light source. The wavelength was between 400 and 800 nm. The intensities of incident beams were checked by a power and energy meter and the light dose used for irradiation was 27 J·cm^{-2}. The experiments were performed in phosphate-buffered saline (PBS, 20 mM) solution. Zeta potentials were measured on a Nano ZS (ZEN3600) system.

Synthesis of Monomer 2. To a solution of 2-(3-thienyl)ethanamine hydrochloride (**1**) (525 mg, 3.20 mmol) in methanol was added dropwise a solution of NaOH (1.28 g, 32.0 mmol) in methanol, and the resulting mixture was stirred at room temperature for 12 h. After removal of the methanol, 5 mL of water was added and the mixture was extracted with CH_2Cl_2. The organic layer was washed with water and dried over anhydrous $MgSO_4$. The solvent was removed and the residue was dissolved in 20 mL of methanol, and then 1.42 mL of methyl acrylate and boric acid (20 mg) in 3 mL of water was added to this solution. After 24 h of stirring at 37 °C, the solvent was removed under vacuum and the residue was purified by silica gel column with petroleum ether/ethyl acetate (4:1) as eluent to yield a colorless oil (538 mg, 56%). ^{1}H NMR (400 MHz, $CDCl_3$, ppm): 7.24−7.22 (m, 1H), 6.96−6.92 (m, 2H), 3.66 (s, 6H), 2.85−2.82 (t, 4H), 2.78−2.75 (t, 2H), 2.71−2.68 (t, 2H),

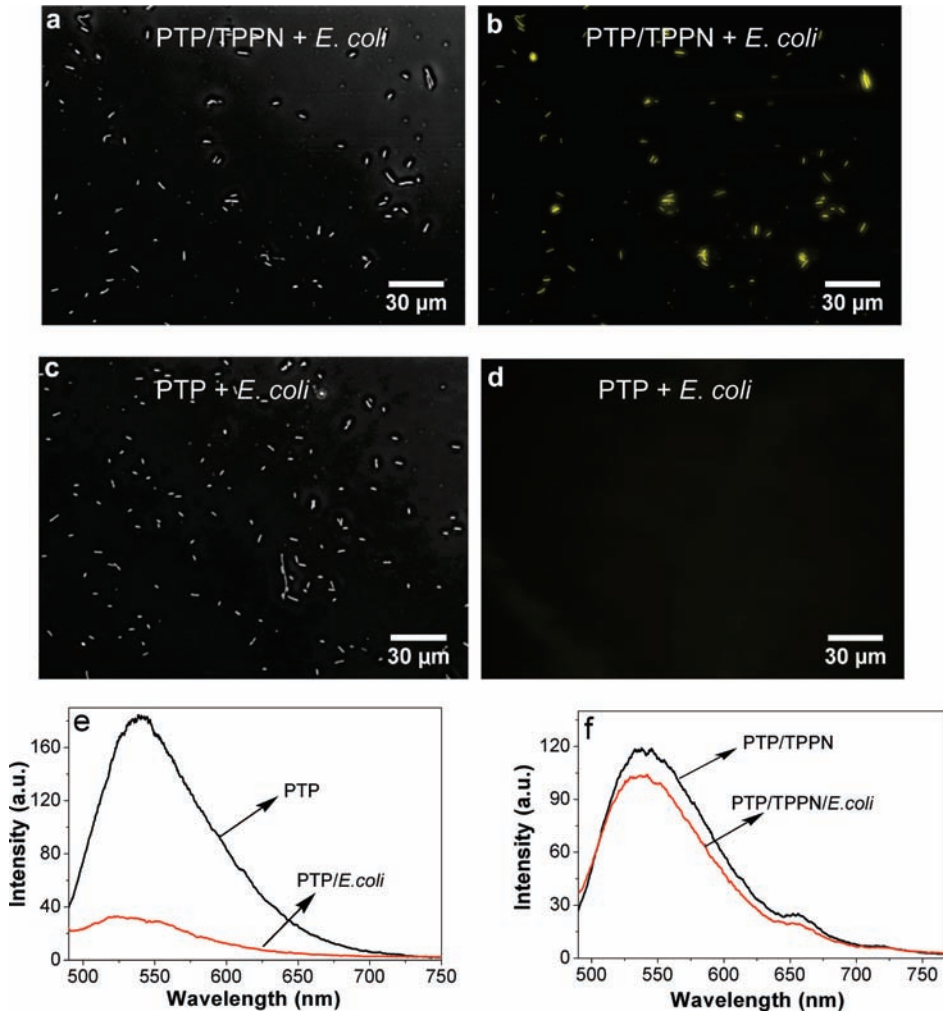

Figure 6. Binding abilities of PTP and PTP/TPPN to *E. coli*: phase-contrast images (a, c) and fluorescence microscope images (b, d) of *E. coli* incubated with PTP/TPPN and PTP. [PTP] = 18.0 μM in RUs, [TPPN] = 6.0 μM. The phase-contrast images were taken at 100 ms exposure time and the fluorescence images were taken at 4500 ms exposure time. The false color is yellow and the type of light filter is D455/70 nm exciter, 500 nm beamsplitter, and D525/30 nm emitter. Magnification of object lens is 40×. Also shown are fluorescence emission spectra of (e) PTP and (f) PTP/TPPN incubated with and without interactions with *E. coli* in 2% SDS. Suspensions of *E. coli* in PBS buffer were incubated with PTP and PTP/TPPN at 37 °C for 40 min in the dark ([TPPN] = 3.0 μM, [PTP] = 9.0 μM in RUs). The cultures were centrifuged (4000 rpm for 10 min) and the supernatant was removed. The bacterial pellet was suspended in 2 mL of 2% SDS, incubated overnight at 4 °C, and then sonicated for 30 min at room temperature to give a homogeneous solution; the fluorescence spectra of the samples were then measured. Fluorescence emission spectra of PTP and PTP/TPPN without *E. coli* in 2% SDS were taken as controls for comparison.

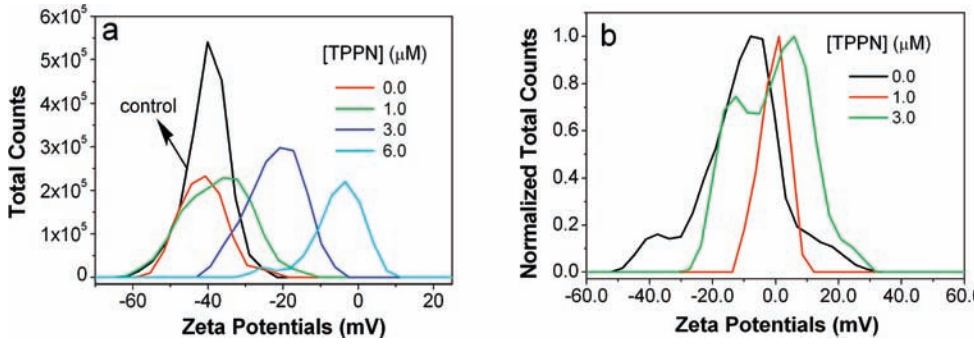

Figure 7. ζ potentials of PTP/TPPN (a) with *E. coli* or (b) without *E. coli* in phosphate-buffered saline (PBS, 20 mM, pH 7.4) solution. [PTP] = 9.0 μM, [TPPN] = 0−6.0 μM. Control plot was carried out with *E. coli* only in panel a.

2.47−2.43 (t, 4H). ^{13}C NMR (100 MHz, $CDCl_3$, ppm): 171.7, 139.4, 127.3, 124.0, 119.6, 53.6, 50.3, 48.2, 31.5, 27.1. MS (EI): m/z = 300 ($[M + H]^+$). $C_{14}H_{21}NO_4S$: calcd C 56.16, H 7.07, N 4.68; found C 56.52, H 7.02, N 4.74.

Synthesis of PTP. A suspension of anhydrous $FeCl_3$ (305 mg, 1.887 mmol) in 10 mL of $CHCl_3$ was stirred for 30 min at room temperature under N_2. To this suspension was added a solution of monomer **2** (142 mg, 0.472 mmol) in 3 mL of $CHCl_3$, and the

resulting solution was stirred for 2 days at room temperature. After the reaction was quenched by the addition of methanol, the precipitate was filtered off and the pellet was washed by CH_3OH/CH_3Cl_3 (1:1). The precipitate was dissolved in 3 mL of dimethyl sulfoxide (DMSO), and a solution of NaOH (0.4 g) in 3 mL of H_2O was added. The mixture was stirred at 50 °C for 12 h and then dialyzed through a membrane with a molecular weight cutoff of 3500 for 2 days to yield 40 mg of PTP. ^{1}H NMR (400 MHz, DMSO-d_6, ppm): 11.80−11.57 (br s), 8.50−8.22 (br s), 7.60−7.47 (br s), 3.60−3.29 (br s), 3.00 (br s), 2.59 (br s).

Synthesis of 5,10,15,20-Tetrakis[4-(6-bromohexyloxy)phenyl]porphyrin (4). The mixture of pyrrole (1.64 mmol) and 4-(6-bromohexyloxy)benzaldehyde (**3**) (468 mg, 1.64 mmol) in 100 mL of $CHCl_3$ was stirred for 15 min under nitrogen at room temperature, and then BF_3−diethyl ether (0.408 mmol) was added to this solution. After 2 h of stirring, DDQ (280 mg, 1.225 mmol) was added and the reaction mixture was stirred for a further 2 h at room temperature. The solvent was removed and the residue was purified by silica gel chromatography with $CHCl_3$/petroleum ether (1:5) as the eluent to afford a purple powder (66 mg, 12%). ^{1}H NMR (400 MHz, $CDCl_3$, ppm): 8.86−8.52 (d, 8H), 8.09−7.84 (d, 8H), 7.28−7.26(d, 4H), 6.99−6.97 (d, 4H), 4.24−4.06 (t, 8H), 3.51−3.43 (t, 8H), 2.05−1.91 (m, 16H), 1.84−1.67 (m, 16H), −2.75(s, 2H). ^{13}C NMR (100 MHz, $CDCl_3$, ppm): 191.3, 164.6, 159.3, 136.1, 135.0, 132.5, 130.3, 120.3, 115.2, 113.2, 68.6, 34.2, 33.1, 29.4, 28.3, 25.7. MS (MALDI-TOF): m/z = 1331 (M). $C_{68}H_{74}Br_4N_4O_4$: calcd C 61.36, H 5.60, N 4.21; found C 60.81, H 6.05, N 3.38.

Synthesis of 5,10,15,20-Tetrakis[4-(6-*N*,*N*,*N*-trimethylammoniumhexyloxy)phenyl]porphyrin Bromide (TPPN). To solution of compound **4** (20 mg, 0.015 mmol) in THF/$CHCl_3$ was added dropwise 3 mL of 30% trimethylamine−water solution, and the solution was stirred at 42 °C for 24 h. Excessive trimethylamine and the solvent were removed under reduced pressure, the residue was dissolved in 1.0 mL of CH_3OH, and 10 mL of hexane was added to precipitate the product as a purple solid (17 mg, 72%). ^{1}H NMR (400 MHz, CD_3OD, ppm): 8.50 (s, 8H), 7.77−7.72 (t, 8H), 6.98−6.96(d, 4H), 6.92−6.90 (d, 4H), 3.86−3.84 (t, 8H), 3.29−3.27 (m, 44H), 1.76−1.69 (m, 16H), 1.46−1.28 (m, 16H), −2.80 (s, 2H). ^{13}C NMR (100 MHz, CD_3OD, ppm): 190.4, 167.5, 163.4, 158.0, 134.2, 132.7, 130.0, 126.5, 118.9, 113.5, 111.5, 69.3, 65.3, 57.8, 27.7, 27.4, 24.6, 24.2. MS (ESI): m/z = 312 (M − 4Br).

Singlet Oxygen Measurement. To 300 μL of the solutions of PTP, TPPN, or PTP/TPPN in PBS were added 3 μL of ADPA solution in water (6 mM). D_2O was used to replace H_2O in these experiments. The UV−vis absorption spectra were measured at 1.0 min intervals after the samples were irradiated with white light and the reduction in absorption of ADPA at 378 nm was plotted as a function of the irradiation time.

Bacterial Killing Experiments. A single colony of *E. coli* on a solid Luria−Bertani (LB) agar plate was transferred to 5 mL of liquid LB culture medium in the presence of 50 μg/mL ampicillin and was grown at 37 °C for 12 h. Bacteria were harvested by centrifuging (4000 rpm for 10 min) at 4 °C and washing by PBS three times. The supernatant was discarded and the remaining *E. coli* were resuspended in PBS. The phototoxicity of TPPN, PTP, and PTP/TPPN complex were determined by incubation with *E. coli* cells suspensions for 15 min in the dark at room temperature and then exposure to an optical fiber of 90 mW/cm^2 white light for 5 min (27 J cm^{-2}). The bacterial cells were centrifuged (4000 rpm for 10 min) and the supernatant was removed, and then the bacterial pellet was suspended and serially diluted (6×10^4)-fold in PBS. A 100 μL portion of the diluted bacterial *E. coli* was spread on the solid LB agar plate, and the colonies formed after 12−16 h incubation at 37 °C were counted. The survival fraction was determined by dividing the number of colony-forming units (cfu) of the samples incubated with photosensitizers by the number of cfu of the control that was carried out in the absence of photosensitizers in the dark. Bacterial death assays were also performed by ethidium bromide (EB) staining. EB was added to the samples that had been illuminated by white light, and they were then observed by fluorescence microscopy.

Binding Affinity to *E. coli* Cells for Photosensitizers. Suspensions of *E. coli* in PBS were incubated with PTP or PTP/TPPN complex at 37 °C for 40 min in the dark ([TPPN] = 3.0 μM, [PTP] = 9.0 μM in RUs). The cultures were centrifuged (4000 rpm for 10 min) and the supernatant was removed. The bacterial pellet was suspended in 2 mL of 2% SDS, incubated overnight at 4 °C, and then sonicated for 30 min at room temperature to afford a homogeneous solution. The fluorescence emission spectra of the samples were measured. Emission spectra of PTP and PTP/TPPN complex without *E. coli* were taken as controls for comparisons.

Acknowledgment. We are grateful for financial support from the National Natural Science Foundation of China (20725308, 20721061, and TRR61), the National Basic Research Program of China (2006CB806200), and the Major Research Plan of China (2006CB932100).

JA904492X